



OPEN

Metformin inhibits the growth of SCLC cells by inducing autophagy and apoptosis via the suppression of EGFR and AKT signalling

Hong Xia^{1,5}, Xue-jiao Tai^{1,5}, Wang Cheng^{1,5}, Yi Wu², Dan He³, Li-feng Wang³, Hao Liu¹, Shen-yi Zhang¹, Yu-ting Sun¹, Hang-zhi Liu¹, Dan-dan Liu¹, Hu-zi Zhao¹, Fu-yun Ji^{1,4}✉ & Xi-hua Li¹✉

Small cell lung cancer (SCLC) is a therapeutically challenging disease. Metformin, an effective agent for the treatment of type 2 diabetes, has been shown to have antitumour effects on many cancers, including non-small cell lung cancer (NSCLC) and breast cancer. Currently, the antitumour effects of metformin on SCLC and the underlying molecular mechanisms remain unclear. CCK-8, EdU, colony formation, flow cytometry, immunofluorescence, molecular docking, western blotting, nude mouse transplanted tumour model, and immunohistochemistry experiments were conducted to analyse gene functions and the underlying mechanism involved. In vitro experiments demonstrated that metformin inhibited the growth of SCLC cells (H446, H526, H446/DDP and H526/DDP), which was confirmed in xenograft mouse models in vivo. Additionally, metformin induced cell cycle arrest, apoptosis, and autophagy in these SCLC cells. The molecular docking results indicated that metformin has a certain binding affinity for EGFR. The western blotting results revealed that metformin decreased the expression of EGFR, p-EGFR, AKT, and p-AKT, which could be reversed by EGF and SC79. Moreover, metformin activated AMPK and inactivated mTOR, and compound C and SC79 increased the levels of p-mTOR. Metformin can not only enhance the antitumour effect of cisplatin but also alleviate the toxic effects of cisplatin on the organs of xenograft model animals. In summary, the current study revealed that metformin inhibits the growth of SCLC by inducing autophagy and apoptosis via suppression of the EGFR/AKT/AMPK/mTOR pathway. Metformin might be a promising candidate drug for combination therapy of SCLC.

Keywords SCLC, Metformin, Apoptosis, Autophagy, Cell cycle arrest

Lung cancer was the leading cause of cancer-related death in both China and the United States of America (USA) in 2022¹. Small cell lung cancer (SCLC), an aggressive neuroendocrine tumour derived from bronchial epithelial cells, accounts for approximately 13–15% of newly diagnosed lung cancer cases². Owing to the short doubling time, strong proliferative ability, and early widespread metastasis of tumour cells, 70% of patients with SCLC are in the extensive stage at the time of initial diagnosis³. The standard of care for SCLC is platinum-etoposide chemotherapy. Regrettably, acquired multidrug resistance (MDR) induced by platinum has resulted in a 5-year survival rate of only 5–6% for SCLC patients in the past 30 years⁴. Additionally, although immunotherapy targeting PD-1 or PD-L1 combined with chemotherapy has improved the median overall survival (OS) of extensive-stage SCLC patients to 15.4 months, with a median OS increase of up to 4.5 months⁵, the vast majority of inhibitors of potential therapeutic targets for SCLC have had minimal or no impact on progression-free survival (PFS) or OS^{6,7}.

¹Hubei Key Laboratory of Embryonic Stem Cell Research, School of Basic Medical Science, Hubei University of Medicine, 30 Renmin Road, Shiyan 442000, Hubei, China. ²Department of Oncology, Taihe Hospital, Hubei University of Medicine, 30 Renmin Road, Shiyan 442000, Hubei, China. ³School of Biomedical Engineering, Hubei University of Medicine, 30 Renmin Road, Shiyan 442000, Hubei, China. ⁴Yu-Yue Pathology Scientific Research Center, 313 Gaoteng Avenue, Jiulongpo District, Chongqing 400039, China. ⁵Hong Xia, Xue-jiao Tai and Wang Cheng contributed equally to this work. ✉email: jifuyun@263.net; jifuyun@jblab.ac.cn; 20180503@hbmhu.edu.cn; lixh87@126.com

To address bottlenecks related to the development of anticancer drugs and improve survival in cancer patients, drug repositioning has become a new and effective method for exploring and developing therapeutic drugs in depth. One repurposed drug is metformin (N, N-dimethylbiguanide). Metformin, derived from galegine, was initially used as a first-line oral therapy for type 2 diabetes (T2D), mainly because of its ability to suppress hepatic gluconeogenesis⁸. Metformin has been reported to delay ageing and play critical roles in ageing-related diseases (such as Alzheimer's disease, cardiovascular diseases, and osteoarthritis)^{9,10}, chronic immune-inflammatory diseases¹¹, and even COVID-19¹². Since it was reported in 2010 that T2D patients had a lower cancer incidence after treatment with metformin¹³, which indicates the anticancer potential of this drug, an increasing number of clinical trials of metformin have been conducted in nondiabetic patients with cancers, including breast cancer and non-small cell lung cancer (NSCLC), and have produced encouraging results^{14,15}. Notably, metformin and EGFR-tyrosine kinase inhibitors (TKIs) have been shown to have synergistic effects in the treatment of diabetic and nondiabetic patients with NSCLC with EGFR mutations¹⁶.

Molecularly, metformin targets adenosine monophosphate-activated protein kinase (AMPK)-dependent/AMPK-independent metabolic pathways, oncogenes/tumour suppressors, and immune pathways that contribute to its anticancer activity¹⁷. For example, metformin reverses the acquired resistance of HCC827 cells with an EGFR mutation (NSCLC) to EGFR-TKIs via the AMPK/ERK/NF- κ B signalling pathway¹⁸. In colorectal cancer, metformin suppresses the growth of tumour cells by inhibiting the TGF- β /PI3K/AKT signalling pathway through an AMPK-independent pathway¹⁹. Interestingly, metformin-induced activation of AMPK can induce the phosphorylation and translocation of p53 to the mitochondria to promote the cisplatin-induced death of A549 cells harbouring wild-type EGFR (NSCLC)²⁰.

The anticancer function of metformin has also been tested in SCLC patients with diabetes; the results revealed that metformin could significantly improve the PFS of this specific subgroup of SCLC patients²¹. Similarly, a patient with SCLC was reported to exhibit an overall partial response after treatment with metformin combined with nivolumab²². Additionally, metformin was shown to enhance the efficacy of figitumumab (an anti-IGF-1R monoclonal antibody) in SCLC cells with high expression of IGF-1R by promoting further IGF-1R downregulation²³. Currently, whether metformin has broad-spectrum anticancer effects on SCLC cells is still unknown, and the anticancer mechanism needs to be further investigated. Therefore, we carried out this study and report that metformin inhibited the growth of both parental SCLC cells (H446 and H526) and cisplatin-resistant SCLC cells (H446/DDP and H526/DDP) by inducing apoptosis and autophagy via inhibition of the EGFR/AKT pathway.

Materials and methods

Chemical reagents

Metformin (M107827, Aladdin, Shanghai, China) with a purity of up to 97% was dissolved in phosphate-buffered saline (PBS) to prepare a 1 M stock solution. The autophagy inhibitor 3-methyladenine (3-MA, HY-19312), the EGFR activator EGF (HY-P70590), the AMPK inhibitor compound C (HY-13418 A), and the AKT activator SC79 (HY-18749) were purchased from MedChemExpress (Shanghai, China).

Generation of cisplatin-resistant cell lines

The human SCLC cell lines H446 and H526 were purchased from the Cell Center of the Chinese Academy of Sciences (Shanghai, China). The cells were cultured in RPMI 1640 medium (SH30809.01, HyClone, New Zealand) supplemented with 10% foetal bovine serum (FBS, SH30406.05, HyClone, New Zealand), 100 U/ml penicillin, and 0.1 mg/mL streptomycin (C0222, Beyotime, Shanghai, China) under standard conditions (37 °C, 5% CO₂). The H446/DDP and H526/DDP cisplatin-resistant cell lines were established and verified as described in our previous studies²⁴.

Cell proliferation assay

For the CCK-8 analysis, cells were seeded in 96-well plates (3×10^3 cells per well) and treated with metformin at different concentrations (0, 2.5, 5, 10, 20, and 40 mM) for 24, 48, or 72 h. The cells were subsequently incubated with 10 μ l of CCK-8 for 1 h. The absorbance values were determined at 450 nm via spectrophotometric measurements with a Spectra Max190 spectrophotometer (Molecular Devices Corp., CA, USA). For the EdU assay, cells were seeded in 24-well plates (3×10^4 cells per well) and incubated with different metformin concentrations (0, 5, and 10 mM) for 48 h. After incubation, the cells were treated with the EdU working solution for 2 h. The cells were subsequently fixed with 4% paraformaldehyde for 15 min at room temperature, followed by permeabilization with 0.5% Triton X-100 for 15 min. The cells were then stained with Click reaction solution in the dark for 30 min and counterstained with Hoechst 33342 for 10 min. The cells were observed and photographed with an IX53 fluorescence microscope (Olympus, Japan). The cells were seeded in 6-well plates (1×10^5 cells per cell) for the colony formation assay. After treatment with metformin for 48 h, the cells were incubated with complete RPMI 1640 medium for 2 weeks. The cells were stained with 0.2% gentian violet, and the colonies were counted under a light microscope. For the above assays, cells were seeded in plates and cultured under standard conditions (37 °C, 5% CO₂) for 24 h before metformin treatment.

Cell cycle assay

The cell cycle distribution was analysed via a Cell Cycle and Apoptosis Analysis Kit (C1052, Beyotime, Shanghai, China). Specifically, 2×10^5 cells per well were seeded in 6-well plates, cultured for 24 h, and then incubated with metformin (0, 5, or 10 mM) for 48 h. The cells, including adherent and suspended dead cells in the culture medium, were harvested and fixed with pre-cooled 75% ethanol overnight at 4 °C. The cells were then stained with propidium iodide (PI) for 30 min in the dark and analyzed by flow cytometry (Cytoflex, Beckman Coulter, USA). Cell cycle distribution was analyzed using ModFit LT4.1 software.

Cell apoptosis analysis

Cell apoptosis was measured via an Annexin V-FITC Apoptosis Detection Kit (C1062; Beyotime, Shanghai, China) according to the manufacturer's instructions. After treatment with different concentrations of metformin (0, 5, or 10 mM) for 48 h, or treatment with 10 mM metformin for 0, 24, 48, or 72 h, the cells were harvested and suspended in 195 μ l of binding buffer and/or Annexin V-FITC (5 μ l) and/or PI (10 μ l). The cell suspension was incubated in the dark for 20 min. The fluorescence intensity was measured via flow cytometry. For each sample, 1×10^4 events were collected. Data from the first and fourth quadrants were used for the column chart shown.

Western blotting

After incubation with different concentrations of metformin, the cells were lysed with RIPA buffer (P0013B, Beyotime, Shanghai, China) containing 1% PMSF (ST506, Beyotime, Shanghai, China). The BCA method was used to determine the protein concentration. Total proteins were separated by 8–15% SDS-PAGE and then transferred to 0.22- or 0.45- μ m PVDF blotting membranes (#10600021 or #10600023, GE Amersham, USA) depending on the molecular weight of the target proteins. The membranes were blocked with 5% nonfat milk for 1 h, cut horizontally at room temperature, and incubated with different primary antibodies separately overnight at 4 °C. The membranes were subsequently incubated with a horseradish peroxidase (HRP)-conjugated secondary antibody (#SA00001-1 or #SA00001-2, Proteintech, Wuhan, China) for 1 h at room temperature. Finally, the bands were detected via a detection system ChemiDoc Touch western blotting detection system (Bio-Rad, USA) with an enhanced chemiluminescence (ECL) test kit (E411, Vazyme, Nanjing, China). The following primary antibodies against the following targets were purchased from Proteintech Group, Inc. (Wuhan, China): β -actin (#66009-1-Ig), Bax (#60267-1-Ig), Bcl-2 (#12789-1-AP), Mcl-1 (#16225-1-AP), caspase 9 (#66169-1-Ig), LC3 (#14600-1-AP), P62 (#18420-1-AP), Beclin1 (#66665-1-Ig), AMPK (#10929-2-AP), AKT (#60203-2-Ig), p-AKT (Ser473) (#66444-1-Ig), mTOR (#66888-1-Ig), and EGFR (#66455-1-Ig). Primary antibodies against the following targets were obtained from Beyotime Biotech. Inc. (Shanghai, China): Cyclin A2 (AF6624), Cyclin D1 (AF1183), Cyclin B1 (AF1606), CDK1 (AF0111), CDK2 (AF1063), and CDK6 (AF0114). Primary antibodies against p-AMPK α (Thr172) (#2535S), p-mTOR (Ser2448) (#5536S), and p-EGFR (Tyr1068) (#3777S) were obtained from Cell Signaling Technology (CST) (Shanghai, China).

Immunofluorescence analysis

A total of 2×10^4 cells per well were seeded in confocal Petri dishes and cultured for 24 h prior to incubation with or without metformin (0 and 10 mM, respectively) for 48 h. Then, the cells were fixed with 4% paraformaldehyde for 30 min, permeabilized with 0.5% Triton X-100 for 10 min, and blocked with 5% BSA for 1 h at room temperature. After incubation with the primary antibody against LC3 overnight at 4°C, the cells were treated with an Alexa Fluor 488-labelled goat anti-rabbit IgG (H + L) secondary antibody (A0423, Beyotime, Shanghai, China) for 1 h, followed by staining with DAPI for 5 min. The images were captured by an FV3000RS laser scanning confocal microscope (OLYMPUS, Japan).

ATP content assay

ATP content was evaluated with an ATP assay kit (S0026, Beyotime, Shanghai, China). After treatment with metformin for 48 h, the cells were harvested and fully lysed on ice. The supernatant was subsequently collected for subsequent analysis according to the manufacturer's instructions. The relative light units (RLUs) were measured using a SpectraMax i3x (Molecular Devices, USA). The concentration of ATP in each sample was calculated according to the standard curve.

Molecular docking

The tyrosine kinase domain structure of EGFR (PDB code: 1M14) was obtained from the RCSB PDB database (<https://www.rcsb.org/structure/1M14>). The chemical structure of metformin was obtained from the PubChem database (<https://pubchem.ncbi.nlm.nih.gov/#query=metformin>). AutoDock 4.2 was used to convert the compound and core protein pdb files into pdbqt files to search for the active pocket. Finally, AutoDockTools was used to perform the molecular docking.

Animal experiments

Four-week-old female BALB/c-nu mice (Beijing Vital River Laboratory Animal Technology Co., Ltd., China) were used to evaluate the antitumour effects of metformin *in vivo*. The study was reported in accordance with the ARRIVE (Animal Research: Reporting of *In Vivo* Experiments) guidelines. All operations and treatments were designed to minimize animal suffering. All the experimental procedures and protocols were reviewed and approved by the Experimental Animal Ethics Committee of the Hubei University of Medicine [Grant No. 2022-No.035] prior to the initiation of the experiment. All methods were performed in accordance with the relevant guidelines and regulations. Humane endpoint criteria were defined as follows: (i) body weight loss persisted above 20% of the per-dose weight; and (ii) tumour size exceeded 2,000 mm³. The cells were injected subcutaneously into the right anterior armpit of the mice (1×10^6 cells/mouse). When the tumour volume reached 100 mm³, the mice were randomly assigned to four groups (the saline, metformin, cisplatin, and metformin + cisplatin groups, $n = 5$ in each group). The control and metformin groups were orally administered saline or metformin (250 mg/kg), respectively, every day. The cisplatin group was treated with cisplatin (4 mg/kg) through intraperitoneal injection every three days, and the metformin + cisplatin group received oral administration of metformin every day and intraperitoneal administration of cisplatin every three days. The mice were monitored for tumour volume (mm³, length \times width² \times 0.5) and body weight every three days. After treatment for 21 days, all the animals were euthanized by excessive isoflurane anaesthesia at the Experimental Animal Center of Hubei University of Medicine. Xenograft tumours and organs (including the heart, liver, lung, spleen, and kidney) were collected

surgically and fixed in formalin for haematoxylin and eosin (H&E) staining and immunohistochemistry (IHC) analyses. Tumour weights were recorded after the tumours were removed from the mice.

Histopathology scoring

The fixed organs were embedded in paraffin and sectioned at a thickness of 5 μ m for H&E staining. The panoramic images of these sections were scanned using the Motic Digital Slide Assistant System Lite 1.0 and 5 fields were randomly selected at 200 \times magnification for histopathology scoring, conducted in a blinded manner to insure objectivity. Lung injury scores were assessed according to the following categories: neutrophil infiltration, interstitial edema, haemorrhage, and hyaline membrane formation, necrosis, congestion. Each category was rated on a scale of 0–4, with criteria as follows: 0 (Normal); 1 (Minimal, <25% of tissue affected); 2 (Mild, 25–50%); 3 (Moderate, 50–75%); and 4 (Severe, >75%). Scores for each category were summed to produce an overall lung injury score for each section as described in prior studies^{25,26}. Liver pathology was evaluated based on the average number of inflammatory foci observed in non-overlapping fields at 200 \times magnification, with scores assigned as follows: 0 (Normal); 1 (1–3 foci); 2 (4–7 foci); and 3 (>7 foci)²⁷.

IHC staining

IHC was performed on paraffin-embedded sections (thickness, 5 μ m) of the xenograft tumours. After antigen retrieval, a polymer detection system (PV-9000, ZSGB-BIO, Beijing, China) was used for staining. The slides were blocked with goat serum (ZLI-9022, ZSGB-BIO, Beijing, China) and incubated with primary antibodies against p-AMPK (1:100) or Ki-67 (1:500) (ZM-0167, ZSGB-BIO, Beijing, China) overnight at 4 °C. After incubation with an enzyme-conjugated secondary antibody and DAB chromogenic fluid, the slides were stained with haematoxylin staining solution. The images were scanned by a Motic Digital Slide Assistant System Lite 1.0. The IHC score was evaluated via the semiquantitative Remmele scoring system.

Statistical analysis

The data were analysed via GraphPad Prism software (San Diego, CA, USA). The density of the western blot bands was quantified via ImageJ. In vitro experiments were performed three times independently, and the results are presented as the means \pm standard deviations (SDs). Statistically significant differences between groups were examined by one-way analysis of variance (ANOVA) or Student's *t* test. *P* < 0.05 was considered to indicate a statistically significant difference.

Results

Metformin inhibits the growth of SCLC cells in vitro

As shown in Fig. 1A, metformin inhibited the growth of both parental and cisplatin-resistant cells in a time- and dose-dependent manner. The 50% growth-inhibitory concentration (IC_{50}) of metformin in H446 cells was greater than that in H446/DDP cells (10.81 ± 0.74 mM vs. 7.19 ± 0.16 mM, *p* = 0.014). In contrast, the IC_{50} of metformin in H526 cells was lower than that in H526/DDP cells (7.71 ± 0.40 mM vs. 10.86 ± 0.13 mM, *p* = 0.003). Colony formation assays revealed that metformin inhibited the colony formation ability of SCLC cells (Fig. 1B). Additionally, exposure to metformin for 48 h inhibited the proliferation of SCLC cells in a dose-dependent manner (Fig. 1C). These results suggest that metformin could suppress the viability, colony formation, and proliferation of SCLC cells in vitro.

Metformin induces cell cycle arrest in SCLC cells

The cell cycle distribution was assessed via flow cytometry. As shown in Fig. 2A, the cell cycle of H446 cells was arrested in the G1 phase, whereas that of H446/DDP cells was arrested in the S phase after metformin treatment. The cell cycle of H526 and H526/DDP cells arrested in the G2/M phase after treatment with metformin. The western blotting results revealed that cyclin D1 and CDK6 were downregulated, whereas cyclin A2 and CDK2 levels did not change significantly in H446 cells after treatment with metformin, confirming that metformin could induce cell cycle blockade in H446 cells at the G1 stage (Fig. 2B). In H446/DDP cells treated with metformin, cyclin A2 and CDK2 were downregulated, confirming that metformin could induce S-phase cell cycle arrest in H446/DDP cells (Fig. 2B). Cyclin A2 and CDK2 expression was increased, whereas CDK1 expression was decreased in H526 and H526/DDP cells after metformin treatment, confirming that metformin could arrest the cell cycle of H526 and H526/DDP cells in the G2/M phase (Fig. 2C). These results demonstrate that metformin could cause cell cycle arrest at different phases in different SCLC cell lines.

Metformin induces SCLC cell apoptosis and autophagy

As shown in Fig. 3A and Supplementary Figure S1, metformin induced cell death in SCLC cells in a dose- and time-dependent manner. To explore the cell death programs induced by metformin in SCLC cells, several canonical markers of cell death programs, including apoptosis, autophagy, and pyroptosis, were detected via western blotting. As shown in Fig. 3B and C, the antiapoptotic proteins Bcl-2 and Mcl-1 were downregulated, while the proapoptotic protein Bax and the apoptotic executor protein cleaved caspase 9 were upregulated in SCLC cells after treatment with metformin, indicating that metformin could induce apoptosis in SCLC cells. Moreover, LC3-II and Beclin-1 were upregulated, while p62 was downregulated in SCLC cells after treatment with metformin in a dose- and time-dependent manner (Fig. 4A and B), suggesting that metformin could also induce autophagy in SCLC cells, as verified by the immunofluorescence staining of LC3 in SCLC cells (Fig. 4C). The autophagy inhibitor 3-MA reduced the level of LC3-II while increasing the level of p62 (Fig. 4D), confirming that autophagy was activated by metformin in SCLC cells. The expression levels of the pyroptosis-related proteins GSDMD and GSDME were not significantly different between cells treated with metformin and

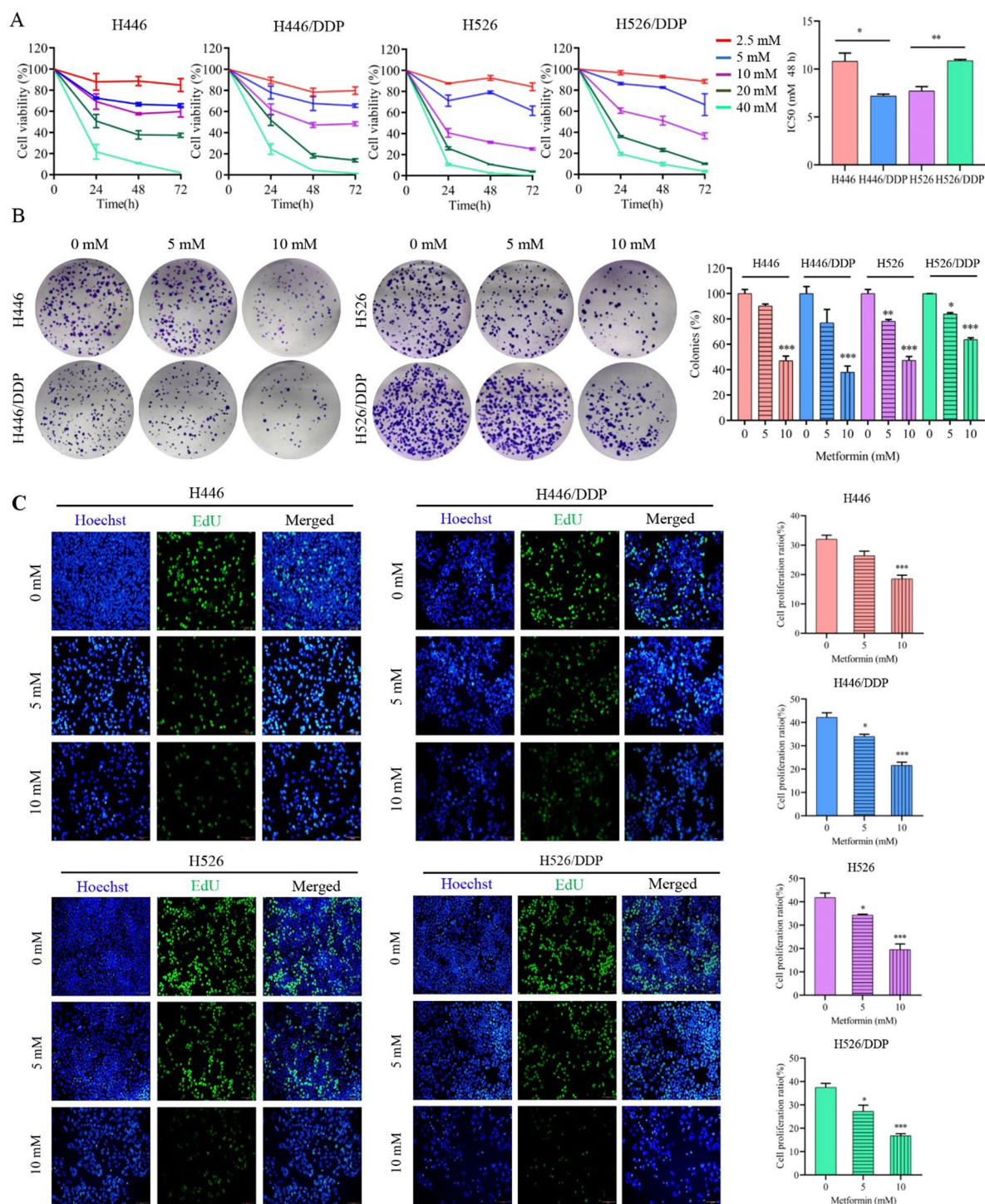


Fig. 1. Metformin inhibits the viability, colony formation, and proliferation of SCLC cells in vitro. **(A)** The viability of H446, H446/DDP, H526 and H526/DDP cells was assessed after treatment with various concentrations of metformin (0, 2.5, 5, 10, 20, and 40 mM) via a CCK-8 assay. The IC₅₀ of metformin (in mM) after 48 h of treatment was determined. **(B,C)** The colony formation **(B)** and proliferation **(C)** of H446, H446/DDP, H526 and H526/DDP cells were evaluated after treatment with various concentrations of metformin (0, 5, and 10 mM, respectively). The error bars indicate the standard deviation (SD). Significant difference compared with the untreated control: * $p < 0.05$; ** $p < 0.01$; *** $p < 0.001$.

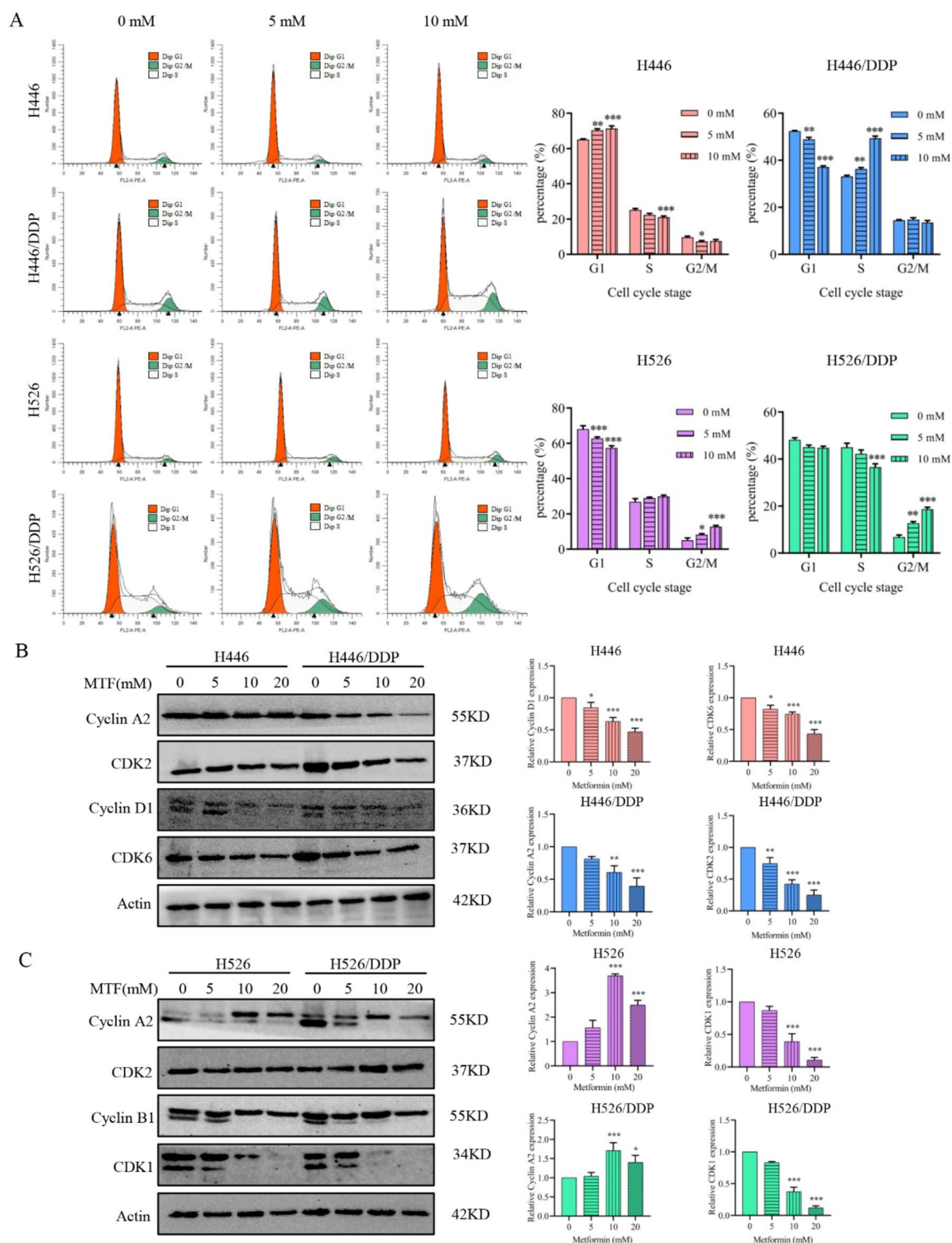


Fig. 2. Metformin blocks the cell cycle of SCLC cells. **(A)** The cell cycle distribution of SCLC cells was detected by flow cytometry. The cells were treated with different concentrations of metformin (0, 5, and 10 mM) for 48 h. The data are presented as the means \pm SDs of values from three independent experiments. $*p < 0.05$; $**p < 0.01$; $***p < 0.001$ compared with the control group. **(B,C)** The expression levels of cell cycle-related proteins were determined by western blotting in H446, H446/DDP **(B)**, H526, and H526/DDP cells **(C)** after treatment with metformin (MTF). Pixel density analysis of protein expression compared with that in the untreated control groups (set to 1). Significant difference compared with the untreated control: $*p < 0.05$; $**p < 0.01$; $***p < 0.001$. $n = 3$.

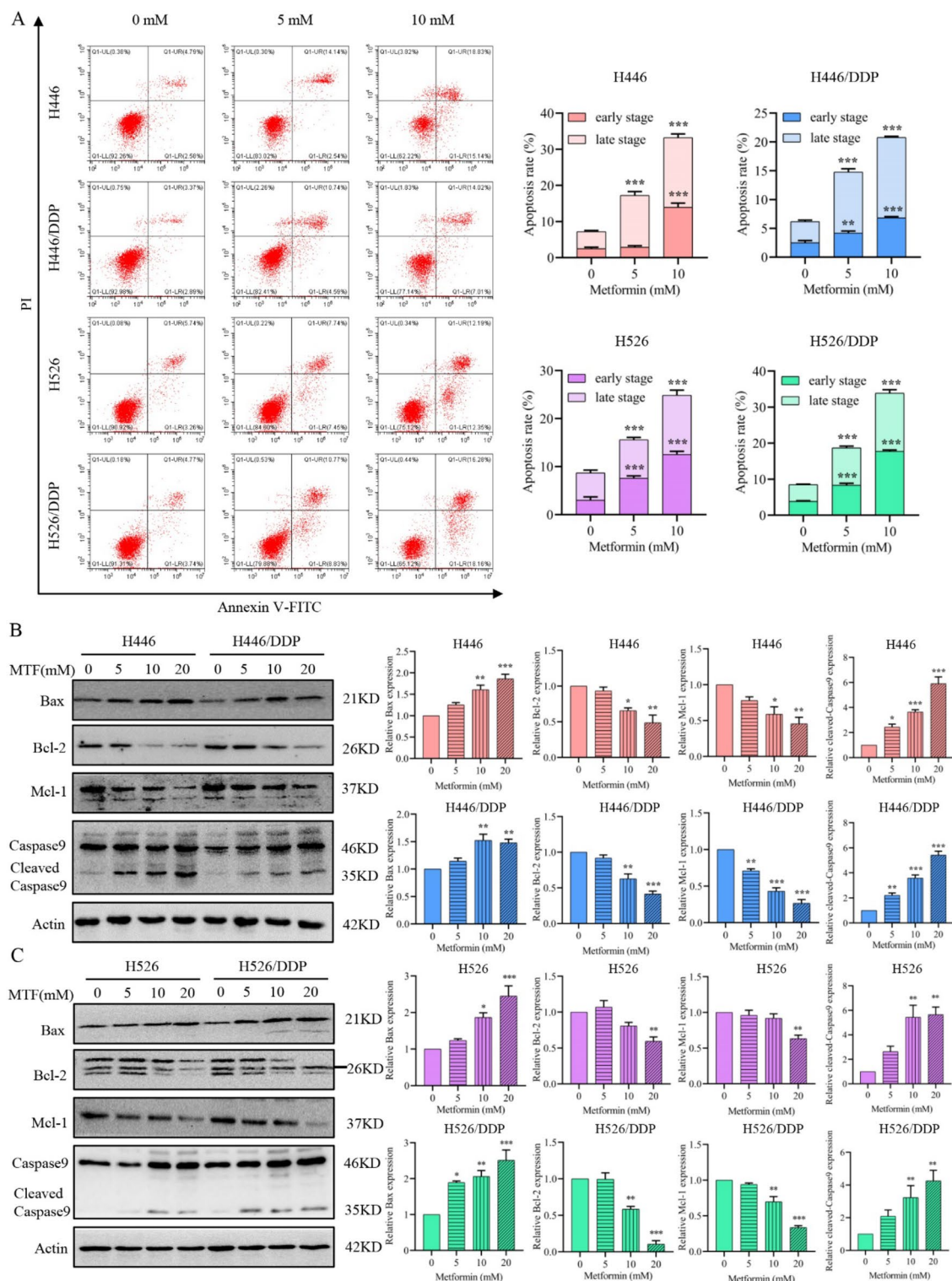


Fig. 3. Metformin promotes SCLC cell apoptosis in a dose-dependent manner. **(A)** Apoptosis rates were measured via flow cytometry via an Annexin V-FITC Apoptosis Detection Kit. The cells were treated with different concentrations of metformin (0, 5, and 10 mM) for 48 h. The data are shown as the means \pm SDs of values from triplicate experiments. * $p < 0.05$; ** $p < 0.01$; *** $p < 0.001$ versus the control group. **(B,C)** Western blotting analysis was conducted to detect the expression levels of apoptosis-related proteins, including Bax, Bcl-2, Mcl-1, and total and cleaved caspase 9, in H446, H446/DDP **(B)**, H526, and H526/DDP **(C)** cells treated with different concentrations of metformin (0, 5, 10, and 20 mM) for 48 h. Pixel density analysis of protein expression compared with that in the untreated control groups (set to 1). Significant difference compared with the untreated control: * $p < 0.05$; ** $p < 0.01$; *** $p < 0.001$. $n = 3$.

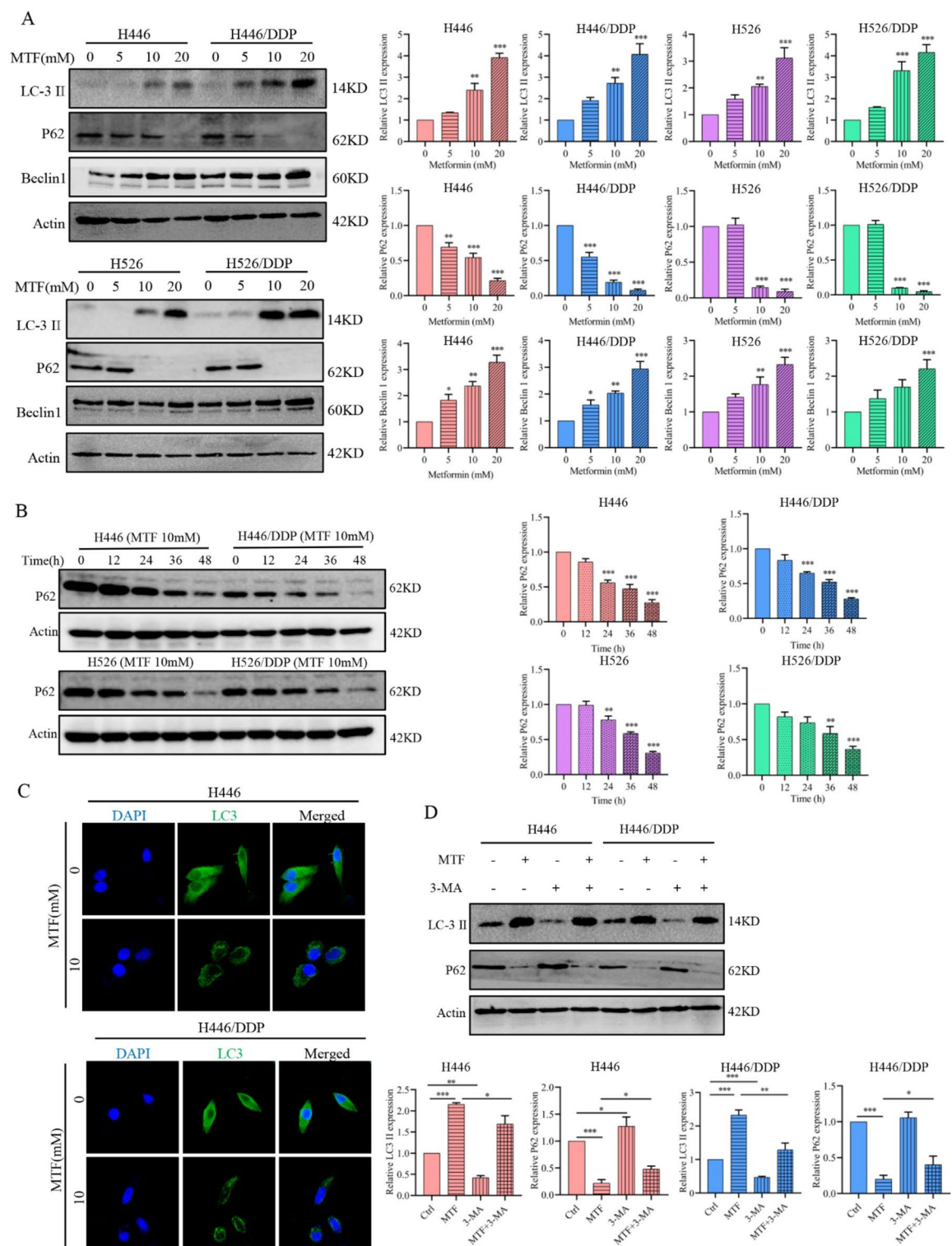


Fig. 4. Metformin activates autophagy in SCLC cells. **(A)** Autophagy-related proteins, including LC3, P62, and Beclin1, were detected by western blotting after H446, H446/DDP, H526, and H526/DDP cells were treated with different concentrations of metformin (0, 5, 10, and 20 mM) for 48 h. **(B)** The protein levels of p62 were detected by western blotting after the cells were treated with 10 mM metformin for 12, 24, 36, or 48 h. **(C)** Immunofluorescence analysis of LC3 in H446 and H446/DDP cells treated with or without metformin for 48 h. The LC3 protein was labelled green (Alexa 488), and the nuclei were labelled blue (DAPI). **(D)** The expression of LC3 and p62 was examined in H446 and H446/DDP cells after treatment with 3-MA (5 mM) combined with metformin (10 mM) for 48 h. Significant difference compared with the untreated control: * $p < 0.05$; ** $p < 0.01$; *** $p < 0.001$. $n = 3$.

control cells (see Supplementary Fig. S2). These results indicate that metformin induces SCLC cell death via apoptosis and autophagy.

Metformin suppresses the EGFR/AKT/AMPK/mTOR axis in SCLC cells

Because metformin reportedly sensitizes NSCLC cancer cells to EGFR-TKIs¹⁶ and prostate cancer cells to radiation through the EGFR signalling pathway²⁸, we detected the levels of EGFR and p-EGFR (Tyr1068) in SCLC cells after treatment with metformin. As shown in Fig. 5A and Supplementary Figure S3, the expression of EGFR and p-EGFR (Tyr1068) decreased in SCLC cells after metformin treatment. To explore the underlying mechanism, AutoDock 4.2 was used to conduct molecular docking analysis of metformin and EGFR. As shown in Fig. 5B, metformin could bind to EGFR via GLU-738 (hydrogen bonds), THR-830 (hydrogen bonds), and ASP-831 (hydrogen bonds and salt bridges). These sites are located in the tyrosine kinase region (amino acids 682–958) of EGFR, which has ATP binding sites that are involved in the activation of downstream signalling pathways²⁹. The binding energy between metformin and EGFR was -4.40 kcal/mol. These results indicate that metformin has a certain binding affinity for EGFR and might be a potential inhibitor of EGFR.

As metformin can regulate autophagy by activating AMPK and inhibiting mTOR by decreasing ATP content and subsequently increasing the AMP/ATP ratio^{30,31}, the ATP content and levels of AMPK/mTOR pathway-related proteins were measured in SCLC cells after treatment with metformin. As shown in Fig. 5C, the ATP content decreased dramatically in SCLC cells treated with metformin. As presented in Fig. 5A and Supplementary Figure S3 online, after the cells were treated with metformin, the levels of p-AMPK (Thr172) increased, whereas the levels of AMPK, mTOR, p-mTOR (Ser2448), AKT, and p-AKT (Ser473) decreased, indicating that metformin could activate the AMPK pathway by promoting the phosphorylation of AMPK at Thr172.

To confirm the role of EGFR in the growth-inhibitory effects of metformin on SCLC cells, EGF was used to activate EGFR. As shown in Fig. 5D and Supplementary Figure S4, EGFR and p-EGFR levels were decreased in cells treated with metformin but increased in cells treated with EGF or EGF combined with metformin, with upregulation of AKT and downregulation of AMPK. Because AKT and p-AKT levels decreased with metformin treatment, SC79 (an AKT activator) was utilized to conduct rescue experiments. As shown in Fig. 5E and Supplementary Figure S5, the AKT, p-AKT, mTOR, and p-mTOR levels were increased, whereas the p-AMPK level was decreased in SCLC cells treated with the combination of metformin and SC79 compared with those treated with metformin only, confirming that AKT is the upstream regulator of mTOR and AMPK. Additionally, the specific AMPK inhibitor compound C was used to attenuate AMPK activation by metformin in SCLC cells. As shown in Fig. 5F and Supplementary Figure S6, the level of p-AMPK was decreased, whereas that of p-mTOR was increased in SCLC cells treated with a combination of metformin and compound C compared with cells treated with metformin alone. These data indicate that metformin exerts anticancer effects on SCLC via the EGFR/AKT/AMPK/mTOR axis.

Metformin suppressed the growth of SCLC in xenograft models

Subcutaneous xenograft models were generated to explore the growth inhibitory effect of metformin on SCLC tumour cells *in vivo*. After treatment with saline, metformin, cisplatin, or metformin combined with cisplatin for 3 weeks, the tumours were resected from the mice. As shown in Fig. 6A–C,E–G, the tumour volumes and weights of the groups treated with metformin, cisplatin, or metformin combined with cisplatin were significantly smaller than those of the group treated with saline (control). There was no significant difference in body weight between the saline group and the metformin group, while the body weight in the groups treated with cisplatin or treated with metformin combined with cisplatin was lower than that in the control group and the groups treated with metformin during the entire experimental process (Fig. 6D,H).

HE staining revealed that the main characteristics of the tumour cells in the xenograft models included the presence of diffuse sheets of small round to fusiform cells with scant cytoplasm and inconspicuous or absent nucleoli with finely granular nuclear chromatin, nuclear chromatin smearing (also called crushed artefacts), and other growth features, such as peripheral palisading, streams, ribbons, organoid nesting, and rosettes. IHC staining with commonly used neuroendocrine staining agents, such as chromogranin A (CGA), synaptophysin (SYN), CD56, and neuron-specific enolase (NSE), revealed that the percentages of cells with positive staining were greater than 90% for all four indicators. HE and IHC staining confirmed that H446 and H526 are SCLC cell lines (see Supplementary Fig. S7). IHC staining for Ki-67 in xenograft tumour tissues demonstrated that the proliferation of tumour cells was inhibited by metformin and promoted by cisplatin. Consistent with the *in vitro* findings, the expression of p-AMPK was increased in the tumour tissues of xenograft models treated with metformin alone or the combination of metformin and cisplatin compared with those of the control groups of SCLC cells (Fig. 6I).

We observed morphological changes in the organs of the experimental mice compared with the normal morphology of the vital organs (such as the heart, liver, spleen, lung, or kidney) in the control saline-treated mice. As shown in Supplementary Fig. S8, metformin did not cause obvious damage to vital organs in the xenograft models. However, the lungs exhibited blood stasis, haemorrhage and inflammation in the group treated with cisplatin and slight haemorrhage in the group treated with metformin combined with cisplatin. Additionally, female BALB/c-nu mice treated with cisplatin exhibited more obvious inflammation than those treated with metformin combined with cisplatin in the liver (Supplementary Fig. S8). These results show that metformin could not only inhibit tumour growth but also alleviate the toxic effects of cisplatin on the organs of xenograft model animals.

Discussion

Metformin, a commonly used antidiabetic drug, has promising effects on inhibiting tumorigenesis and cancer development. However, the mechanism underlying the anticancer effects of metformin in SCLC remains

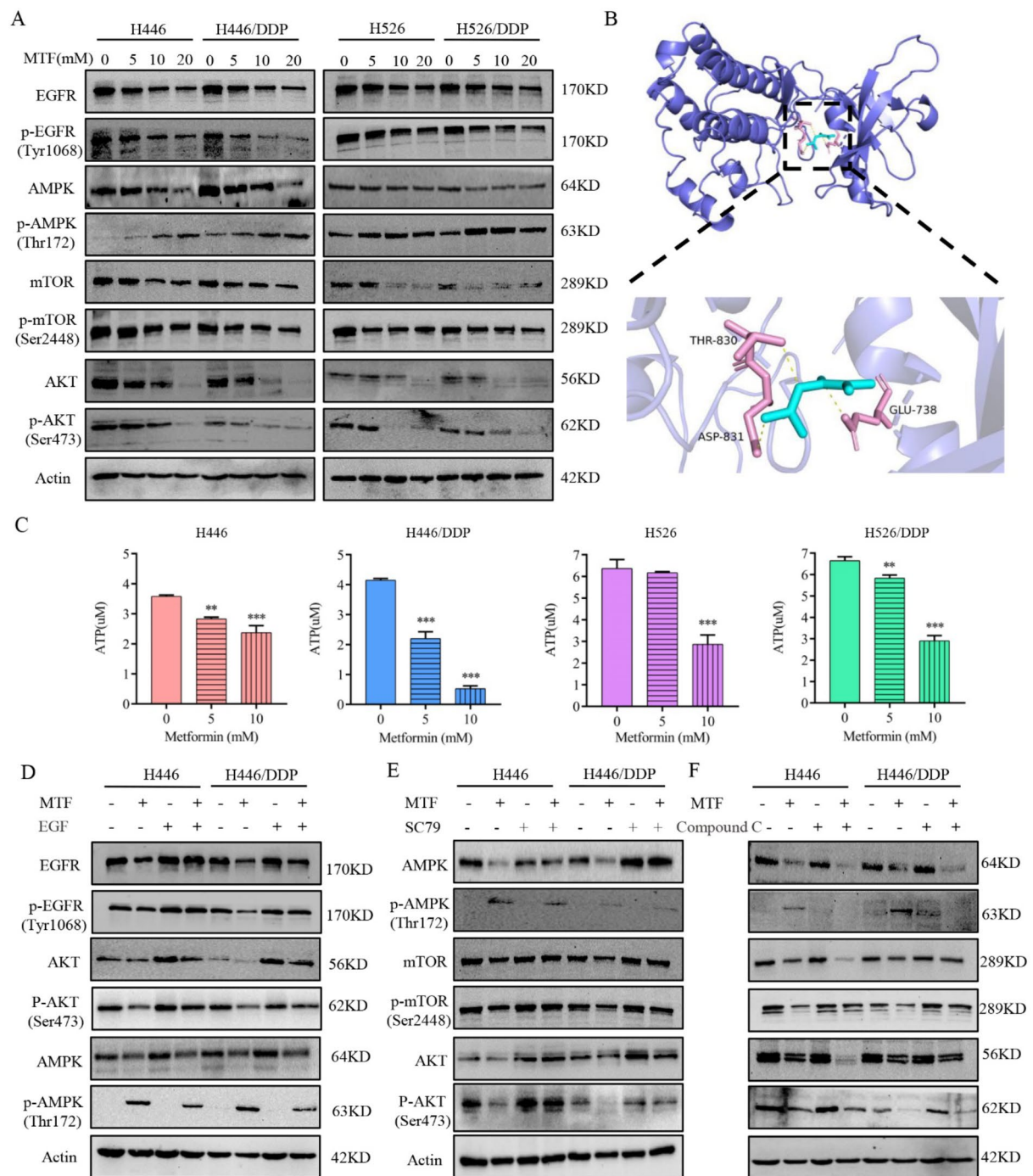


Fig. 5. Metformin inhibits the EGFR/AKT/AMPK/mTOR axis in SCLC cells. **(A)** The protein levels of AMPK, p-AMPK, mTOR, p-mTOR, AKT, p-AKT, EGFR, and p-EGFR were measured in H446, H446/DDP, H526, and H526/DDP cells treated with different concentrations of metformin for 48 h via western blotting. **(B)** The binding mode of metformin docked to EGFR. **(C)** ATP content of SCLC cells after treatment with metformin (0, 5, or 10 mM) for 48 h. Significant difference compared with the untreated control: * $p < 0.05$; ** $p < 0.01$; *** $p < 0.001$. $n = 3$. **(D)** The protein levels of EGFR, p-EGFR, AKT, p-AKT, AMPK, and p-AMPK were measured via western blotting in H446 and H446/DDP cells treated with metformin (10 mM), EGF (50 $\mu\text{g}/\text{ml}$), or metformin + EGF for 48 h. **(E)** The protein levels of AKT, p-AKT, mTOR, p-mTOR, AMPK, and p-AMPK were measured via western blotting in H446 and H446/DDP cells treated with metformin (10 mM), SC79 (4 $\mu\text{g}/\text{ml}$), or metformin + SC79 for 48 h. **(F)** The protein levels of AMPK, p-AMPK, mTOR, p-mTOR, AKT, and p-AKT were measured in H446 and H446/DDP cells treated with metformin (10 mM), compound C (2 μM), or metformin + Compound C for 48 h via western blotting.

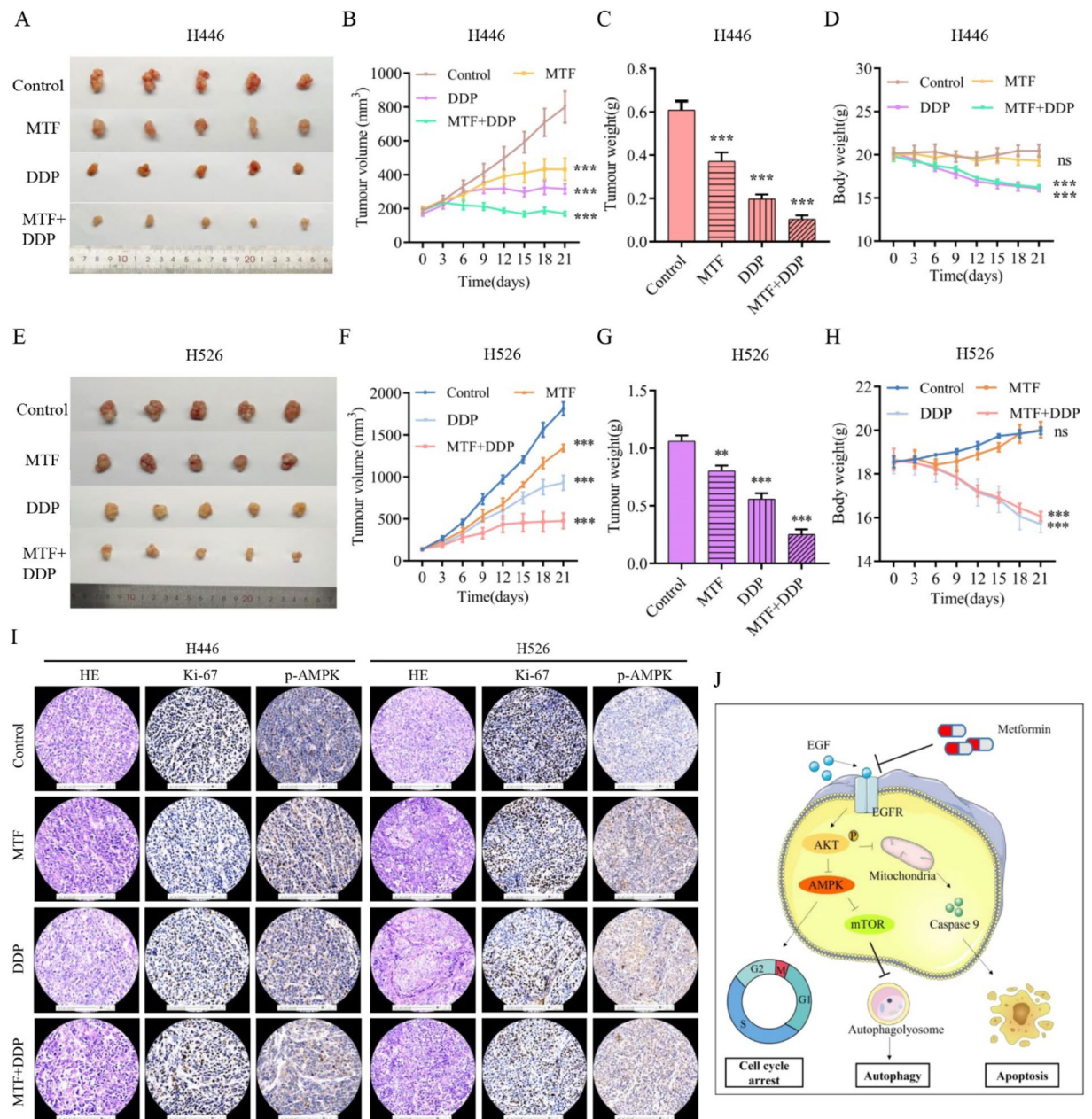


Fig. 6. Metformin inhibits the growth of H446 and H526 cells in vivo. (A,E) Images of isolated tumours from each group after treatment with saline, metformin, cisplatin, or metformin + cisplatin ($n = 5$). (B,F) Growth of the subcutaneous tumours in each group. The tumour volume was calculated on the basis of measurements with a calliper every 3 days. (C,G) The tumour weight in each group was measured after isolation from the female mice. (D,H) The body weights of the female mice after treatment with saline, metformin, cisplatin, or metformin combined with cisplatin for 21 days. Statistical analyses were performed via ANOVA, which revealed significant differences compared with the untreated control: $*p < 0.05$; $**p < 0.01$; $***p < 0.001$. $n = 5$. (I) Images of HE staining and IHC staining (Ki-67 and p-AMPK) of tumour tissues from subcutaneous xenograft models (magnification: $\times 200$). (J) Schematic description of the main molecular mechanism by which metformin suppresses SCLC growth.

unclear. In our study, we found that metformin induced cell death to inhibit the growth of both parental SCLC cells (H446 and H526) and cisplatin-resistant SCLC cells (H446/DDP and H526/DDP).

EGFR can activate prosurvival and antiapoptotic cellular responses by initiating downstream intracellular signalling pathways, including the PI3K/AKT, MAPK, Ras/Raf/MEK/ERK, JAK/STAT3, and PLC γ 1/PKC pathways^{32,33}. Clinical studies have shown that the combination of metformin and EGFR-TKIs delays the onset of resistance, resulting in longer PFS (19.0 vs. 8.0 months, $p = 0.005$) and OS (32.0 vs. 23.0 months, $p = 0.002$) in patients with both type 2 diabetes and NSCLC with EGFR mutations³⁴. Molecularly, metformin can sensitize

NSCLC cells to EGFR-TKI therapy by inhibiting the EGFR signalling pathway³⁵. Additionally, metformin and gefitinib cooperate to inhibit the growth of bladder cancer cells via both the AMPK and EGFR pathways, which interact with AKT and ERK³⁶. Our results showed that metformin can clearly bind to EGFR and decrease the total and phosphorylated levels of EGFR. Consistent with these findings, we also found that metformin exerted antitumour effects in vitro and in vivo and promoted the growth-inhibitory effect of cisplatin on SCLC cells. We found that metformin inhibited the growth of SCLC cells by inhibiting the EGFR signalling pathway.

Metformin can combat cancer by affecting metabolism, epigenetics, the cell cycle, migration, metastasis, cell death, cell senescence, cancer stem cells, immunity, and gut microbes³⁷. It regulates various types of cell death, such as apoptosis, autophagy, pyroptosis, necrosis, and ferroptosis. In our study, to explore the cell death programs induced by metformin in SCLC cells, we detected the expression of autophagy-, apoptosis-, and pyroptosis-related proteins in SCLC cells. Metformin plays a vital role in autophagy through its pharmacological effects, although it has been shown to exert distinctive effects on autophagy in different cancer models³⁰. Previous studies have demonstrated that metformin alone or in combination with other drugs can induce autophagy via different signalling pathways, including the AMPK/mTOR, PI3K/AKT/mTOR, and MAPK/ERK pathways^{38–40}. EGFR is a crucial regulator of autophagy. EGFR can suppress autophagy by binding to beclin-1 to directly inhibit the formation of the vps34/autophagy initiation complex or by indirectly activating the AKT/mTOR pathway^{41,42}. In our work, we found that metformin could activate autophagy by activating AMPK and inhibiting mTOR and AKT, which was reversed by compound C (an AMPK inhibitor) or SC79 (an AKT activator). AKT negatively regulates AMPK by inhibiting the phosphorylation of AMPK at Thr172⁴³. Thus, the finding that SC79 increased the level of p-AKT and decreased the level of p-AMPK suggests that metformin could induce autophagy to inhibit the growth of SCLC via the EGFR/AKT/AMPK/mTOR signalling pathway.

The overexpression or activation of EGFR leads to a poor prognosis for solid tumours due to increased cell proliferation, apoptosis, and autophagy inhibition⁴⁴, indicating the dual role of EGFR in autophagy and apoptosis in cancers. In oesophageal cancer cells, dithiocarbamate induces apoptosis by inhibiting the EGFR/AKT signalling pathway⁴⁵. Combined treatment with triptolide and tyrosine kinase inhibitors enhances H1975 cell (NSCLC) apoptosis through the EGFR/AKT pathway⁴⁶. In this study, metformin increased the expression of Bax and cleaved caspase 9 but decreased the expression of Bcl-2 and Mcl-1 and downregulated the expression of EGFR and AKT in SCLC cells, suggesting that metformin could induce the apoptosis of SCLC cells via the EGFR/AKT/caspase9 pathway.

Autophagy (self-eating) and apoptosis (self-killing) are two self-destructive processes. Crosstalk between autophagy and apoptosis is still an emerging field, and many signalling pathways and molecules, such as RTKs/PI3K/AKT/mTOR and p53, are involved^{47,48}. In this study, we found that metformin could induce autophagy and apoptosis. Excessive autophagy directly leads to autophagic death and autophagy-dependent apoptosis. For example, sodium butyrate induced autophagic apoptosis by blocking AKT/mTOR signalling in nasopharyngeal carcinoma cells⁴⁹. w09, a novel autophagy enhancer, triggers the autophagy-dependent apoptosis of gastric cancer cells via the EGFR/RAS/RAF1/MAP2K/MAPK1/3 pathway⁵⁰. Therefore, we deduced that metformin can trigger autophagy-dependent apoptosis in SCLC.

Metformin has been found to block the cell cycle of tumour cells at different stages by targeting the AMPK pathway^{51,52}. In myeloma cell lines (RPMI8226 and U266), metformin arrested the cell cycle of tumour cells in the G1 phase⁵¹. In breast cancer (MCF-7), NSCLC (A549), and osteosarcoma (U2OS and 143B) cell lines, metformin arrested the cell cycle of tumour cells in the G2/M phase^{52,53}. Similarly, we also found that metformin could induce cell cycle arrest in different phases in SCLC cells by increasing p-AMPK levels. Thus, metformin can block the cell cycle of SCLC tumour cells by upregulating AMPK.

Numerous randomized clinical trials have been conducted to investigate the oncological potential of metformin. However, most results have been disappointing⁵⁴. Many limitations, such as a lack of accurate molecular stratification of patients, insufficient compliance, and a limited study population, may have contributed to these results³⁷. Despite these challenges, some clinical trials have yielded encouraging outcomes. For example, a phase 2 randomized clinical trial that included 139 patients reported that the addition of metformin to standard EGFR-tyrosine kinase inhibitors significantly improved both PFS and OS⁵⁵. Additionally, metformin significantly decreased the number of metastatic cases after 6 months of hormonal therapy⁵⁶. Most importantly, a meta-analysis revealed that metformin improved survival among patients with concurrent SCLC and diabetes⁵⁷. However, the function of metformin in nondiabetic SCLC patients remains unclear. There is also a need to investigate the effects of metformin in patients with both primary and recurrent SCLC. These areas warrant well-designed clinical investigations to determine the broader potential of metformin in SCLC treatment.

For three decades, platinum-based chemotherapy has been the standard therapy for both early-stage SCLC and extensive-stage SCLC, but therapeutic resistance is typically observed. Our findings that metformin inhibits the growth of both parental and cisplatin-resistant SCLC cells in vitro and in vivo strongly suggest the promising clinical application prospects of metformin in SCLC. Additionally, metformin administered at a dosage of 250 mg/kg/day in vivo is equivalent to a dosage of 20.25 mg/kg/day in humans⁵⁸, which is less than the maximum dosage of 2 g/day recommended by the FDA for average adults. Consistent with previous findings, HE staining of heart, liver, spleen, lung, and kidney tissues revealed that metformin, administered at a dosage of 250 mg/kg/day, is safe and effective for the treatment of xenograft models. This aligns with a study on the effects of metformin in human osteosarcoma⁵⁹. Furthermore, the toxicity of cisplatin in mice may be mitigated by the combination of aianthone and cisplatin⁶⁰. In our study, we found that metformin may also attenuate the toxic effects of cisplatin on the organs of xenograft model animals.

As EGFR mutations are rarely observed in SCLC, EGFR-targeted therapies are not commonly used for the treatment of SCLC. Additionally, although PD-1 inhibitors improve the overall survival of patients with extensive-stage SCLC when combined with platinum-based chemotherapy, the benefit is still limited to a minority of patients. Furthermore, resistance emerges relatively rapidly in virtually all patients⁶¹. Thus, our

findings that EGFR is the target of metformin in SCLC provide strong evidence that metformin might be a novel treatment for SCLC through the inhibition of EGFR.

In conclusion, our findings reveal that metformin inhibits the growth of parental and cisplatin-resistant SCLC cells by inducing autophagy and apoptosis through the suppression of the EGFR/AKT/AMPK/mTOR pathway (Fig. 6). Metformin might be a promising candidate option for SCLC therapy.

Data availability

The data that support the findings of this study are available from the corresponding author upon reasonable request.

Received: 29 May 2024; Accepted: 20 January 2025

Published online: 19 February 2025

References

- Xia, C. F. et al. Cancer statistics in China and United States, 2022: profiles, trends, and determinants. *Chin. Med. J.-Peking* **135**, 584–590. <https://doi.org/10.1097/Cm9.0000000000002108> (2022).
- Govindan, R. et al. Changing epidemiology of small-cell lung cancer in the United States over the last 30 years: analysis of the surveillance, epidemiologic, and end results database. *J. Clin. Oncol.* **24**, 4539–4544. <https://doi.org/10.1200/JCO.2005.04.4859> (2006).
- Khan, P. et al. Epigenetic landscape of small cell lung cancer: small image of a giant recalcitrant disease. *Semin. Cancer Biol.* **83**, 57–76. <https://doi.org/10.1016/j.semcancer.2020.11.006> (2022).
- Farago, A. F. & Keane, F. K. Current standards for clinical management of small cell lung cancer. *Transl. Lung Cancer Res.* **7**, 69–79. <https://doi.org/10.21037/tlcr.2018.01.16> (2018).
- Cheng, Y. et al. Effect of first-line serplulimab vs placebo added to chemotherapy on survival in patients with extensive-stage small cell lung cancer: the ASTRUM-005 randomized clinical trial. *JAMA* **328**, 1223–1232. <https://doi.org/10.1001/jama.2022.16464> (2022).
- Mathieu, L. et al. FDA approval summary: Atezolizumab and durvalumab in combination with platinum-based chemotherapy in extensive stage small cell lung cancer. *Oncologist* **26**, 433–438. <https://doi.org/10.1002/onco.13752> (2021).
- Liu, S. V. et al. Updated overall survival and PD-L1 subgroup analysis of patients with extensive-stage small-cell lung cancer treated with atezolizumab, carboplatin, and etoposide (IMpower133). *J. Clin. Oncol.* **39**, 619. <https://doi.org/10.1200/Jco.20.01055> (2021).
- Viollet, B. et al. Cellular and molecular mechanisms of metformin: an overview. *Clin. Sci.* **122**, 253–270. <https://doi.org/10.1042/Cs20110386> (2012).
- Chen, S. et al. Metformin in aging and aging-related diseases: clinical applications and relevant mechanisms. *Theranostics* **12**, 2722–2740. <https://doi.org/10.7150/thno.71360> (2022).
- Deng, M. Y. et al. Metformin and vascular diseases: A focused review on smooth muscle cell function. *Front. Pharmacol.* **11** (2020).
- Sorrenti, V. et al. Immunomodulatory and antiaging mechanisms of resveratrol, rapamycin, and metformin: Focus on mTOR and AMPK signaling networks. *Pharmaceuticals* **15** (2022).
- Ventura-Lopez, C. et al. Treatment with metformin glycinate reduces SARS-CoV-2 viral load: an in vitro model and randomized, double-blind, phase IIb clinical trial. *Biomed. Pharmacother.* **152** (2022).
- Giovannucci, E. et al. Diabetes and cancer: a consensus report. *CA Cancer J. Clin.* **60**, 207–221. <https://doi.org/10.3322/caac.20078> (2010).
- Hassanabad, A. F. & MacQueen, K. T. Molecular mechanisms underlining the role of metformin as a therapeutic agent in lung cancer. *Cell. Oncol.* **44**, 1–18. <https://doi.org/10.1007/s13402-020-00570-0> (2021).
- Ponnusamy, L., Natarajan, S. R., Thangaraj, K. & Manoharan, R. Therapeutic aspects of AMPK in breast cancer: Progress, challenges, and future directions. *BBA-Rev. Cancer* **1874** (2020).
- Wang, H. C. et al. Synergistic effect of metformin and EGFR-TKI in the treatment of non-small cell lung cancer. *Transl. Cancer Res.* **9**, 372–381. <https://doi.org/10.21037/tcr.2019.11.09> (2020).
- Marjanovic, M. S. M., Vucicevic, L. M., Despotovic, A. R., Stamenkovic, M. M. & Janjetovic, K. D. Dual anticancer role of metformin: an old drug regulating AMPK dependent/independent pathways in metabolic, oncogenic/tumorsuppressing and immunity context. *Am. J. Cancer Res.* **11**, 5625–5643 (2021).
- Li, L. et al. Metformin overcomes acquired resistance to EGFR TKIs in EGFR-mutant lung cancer via AMPK/ERK/NF- κ B signaling pathway. *Front. Oncol.* **10** (2020).
- Xiao, Q. et al. Metformin suppresses the growth of colorectal cancer by targeting INHBA to inhibit TGF- β /PI3K/AKT signaling transduction. *Cell Death Dis.* **13** (2022).
- Tortelli, T. C. et al. Metformin-induced chemosensitization to cisplatin depends on P53 status and is inhibited by Jarid1b overexpression in non-small cell lung cancer cells. *Aging-U.S.* **13**, 21914–21940 (2021).
- Cao, X. et al. The clinical effect of metformin on the survival of lung cancer patients with diabetes: a comprehensive systematic review and meta-analysis of retrospective studies. *J. Cancer* **8**, 2532–2541. <https://doi.org/10.7150/jca.19750> (2017).
- Kim, Y. et al. Overcoming acquired resistance to PD-1 inhibitor with the addition of metformin in small cell lung cancer (SCLC). *Cancer Immunol. Immunother.* **70**, 961–965. <https://doi.org/10.1007/s00262-020-02703-8> (2021).
- Cao, H. X. et al. Combinational therapy enhances the effects of anti-IGF-1R mAb figitumumab to target small cell lung cancer. *PLoS ONE* **10** (2015).
- Zhang, R. J. et al. Increased sensitivity of human lung adenocarcinoma cells to cisplatin associated with downregulated contactin-1. *Biomed. Pharmacother.* **71**, 172–184. <https://doi.org/10.1016/j.biopha.2014.11.004> (2015).
- Wang, J. et al. HMGB1 participates in LPS-induced acute lung injury by activating the AIM2 inflammasome in macrophages and inducing polarization of M1 macrophages via TLR2, TLR4, and RAGE/NF- κ B signaling pathways. *Int. J. Mol. Med.* **45**, 61–80. <https://doi.org/10.3892/ijmm.2019.4402> (2020).
- Wang, S., Chen, H., Li, Z., Xu, G. & Bao, X. Hyperbaric oxygen-induced acute lung injury: a mouse model study on pathogenic characteristics and recovery dynamics. *Front. Physiol.* **15**, 1474933. <https://doi.org/10.3389/fphys.2024.1474933> (2024).
- Guo, W. et al. Aloperine suppresses cancer progression by interacting with VPS4A to inhibit autophagosome-lysosome fusion in NSCLC. *Adv. Sci. (Weinh.)* **11**, e2308307. <https://doi.org/10.1002/adv.202308307> (2024).
- Zhang, T. T. et al. Metformin sensitizes prostate Cancer cells to radiation through EGFR/p-DNA-PKCS in vitro and in vivo. *Radiat. Res.* **181**, 641–649. <https://doi.org/10.1667/Rr13561.1> (2014).
- Du, Z. F. & Lovly, C. M. Mechanisms of receptor tyrosine kinase activation in cancer. *Mol. Cancer* **17** (2018).
- Lu, G. L. et al. The effects of metformin on autophagy. *Biomed. Pharmacother.* **137** (2021).
- Vancura, A., Bu, P. L., Bhagwat, M., Zeng, J. & Vancurova, I. Metformin as an anticancer agent. *Trends Pharmacol. Sci.* **39**, 867–878. <https://doi.org/10.1016/j.tips.2018.07.006> (2018).
- Levantini, E., Maroni, G., Del Re, M. & Tenen, D. G. EGFR signaling pathway as therapeutic target in human cancers. *Semin. Cancer Biol.* **85**, 253–275. <https://doi.org/10.1016/j.semcancer.2022.04.002> (2022).

33. Shi, K. et al. Emerging strategies to overcome resistance to third-generation EGFR inhibitors. *J. Hematol. Oncol.* **15**, 94. <https://doi.org/10.1186/s13045-022-01311-6> (2022).
34. Chen, H. Y. et al. Synergistic effects of metformin in combination with EGFR-TKI in the treatment of patients with advanced non-small cell lung cancer and type 2 diabetes. *Cancer Lett.* **369**, 97–102. <https://doi.org/10.1016/j.canlet.2015.08.024> (2015).
35. Cao, F. M. et al. Metformin reverses oxidative stress-induced mitochondrial dysfunction in pre-osteoblasts via the EGFR/GSK-3 β /calcium pathway. *Int. J. Mol. Med.* **51** (2023).
36. Peng, M. et al. Metformin and gefitinib cooperate to inhibit bladder cancer growth via both AMPK and EGFR pathways joining at Akt and Erk. *Sci. Rep.-U.K.* **6** (2016).
37. Hua, Y. et al. Metformin and cancer hallmarks: shedding new lights on therapeutic repurposing. *J. Transl. Med.* **21** (2023).
38. Shi, R. et al. The antileukemia effect of metformin in the Philadelphia chromosome-positive leukemia cell line and patient primary leukemia cell. *Anti-Cancer Drug* **26**, 913–922. <https://doi.org/10.1097/Cad.0000000000000266> (2015).
39. Sun, R. J., Zhai, R. R., Ma, C. L. & Miao, W. Combination of aloin and metformin enhances the antitumor effect by inhibiting the growth and invasion and inducing apoptosis and autophagy in hepatocellular carcinoma through PI3K/AKT/mTOR pathway. *Cancer Med.-U.S.* **9**, 1141–1151. <https://doi.org/10.1002/cam4.2723> (2020).
40. Tomic, T. et al. Metformin inhibits melanoma development through autophagy and apoptosis mechanisms. *Cell Death Dis.* **2** (2011).
41. Wei, Y. J. et al. EGFR-mediated beclin 1 phosphorylation in autophagy suppression, tumor progression, and tumor chemoresistance. *Cell* **154**, 1269–1284. <https://doi.org/10.1016/j.cell.2013.08.015> (2013).
42. Tan, X. J., Lambert, P. F., Rapraeger, A. C. & Anderson, R. A. Stress-Induced EGFR Trafficking: mechanisms, functions, and therapeutic implications. *Trends Cell. Biol.* **26**, 352–366. <https://doi.org/10.1016/j.tcb.2015.12.006> (2016).
43. Zhao, Y. et al. ROS signaling under metabolic stress: cross-talk between AMPK and AKT pathway. *Mol. Cancer* **16** (2017).
44. Zhang, H. T. et al. ErbB receptors: from oncogenes to targeted cancer therapies. *J. Clin. Investig.* **117**, 2051–2058. <https://doi.org/10.1172/Jci32278> (2007).
45. Yang, Y., Tian, Z. Y., Zhao, X. H., Li, Y. & Duan, S. Y. A novel antitumor dithiocarbamate compound inhibits the EGFR/AKT signaling pathway and induces apoptosis in esophageal cancer cells. *Oncol. Lett.* **20**, 877–883. <https://doi.org/10.3892/ol.2020.11638> (2020).
46. Tong, X. P. et al. Combined treatment with triptolide and tyrosine kinase inhibitors synergistically enhances apoptosis in non-small cell lung cancer H1975 cells but not H1299 cells through EGFR/Akt pathway. *Chem. Pharm. Bull.* **67**, 864–871. <https://doi.org/10.1248/cpb.c19-00300> (2019).
47. Booth, L. A., Roberts, J. L. & Dent, P. The role of cell signaling in the crosstalk between autophagy and apoptosis in the regulation of tumor cell survival in response to sorafenib and neratinib. *Semin. Cancer Biol.* **66**, 129–139. <https://doi.org/10.1016/j.semcancer.2019.10.013> (2020).
48. Maiuri, M. C., Zalckvar, E., Kimchi, A. & Kroemer, G. Self-eating and self-killing: crosstalk between autophagy and apoptosis. *Nat. Rev. Mol. Cell. Biol.* **8**, 741–752. <https://doi.org/10.1038/nrm2239> (2007).
49. Huang, W. et al. Sodium butyrate induces autophagic apoptosis of nasopharyngeal carcinoma cells by inhibiting AKT/mTOR signaling. *Biochem. Biophys. Res. Commun.* **514**, 64–70. <https://doi.org/10.1016/j.bbrc.2019.04.111> (2019).
50. Zhang, P. H. et al. w09, a novel autophagy enhancer, induces autophagy-dependent cell apoptosis via activation of the EGFR-mediated RAS-RAF1-MAP2K-MAPK1/3 pathway. *Autophagy* **13**, 1093–1112. <https://doi.org/10.1080/15548627.2017.1319039> (2017).
51. Wang, Y. et al. Metformin induces autophagy and G0/G1 phase cell cycle arrest in myeloma by targeting the AMPK/mTORC1 and mTORC2 pathways. *J. Exp. Clin. Cancer Res.* **37** (2018).
52. Rocha, G. Z. et al. Metformin amplifies chemotherapy-induced AMPK activation and antitumoral growth. *Clin. Cancer Res.* **17**, 3993–4005. <https://doi.org/10.1158/1078-0432.Ccr-10-2243> (2011).
53. Li, B. et al. Metformin induces cell cycle arrest, apoptosis and autophagy through ROS/JNK signaling pathway in human osteosarcoma. *Int. J. Biol. Sci.* **18**, 4468–4468. <https://doi.org/10.7150/ijbs.74954> (2022).
54. Lord, S. R. & Harris, A. L. Is it still worth pursuing the repurposing of metformin as a cancer therapeutic? *Br. J. Cancer* **128**, 958–966. <https://doi.org/10.1038/s41416-023-02204-2> (2023).
55. Arrieta, O. et al. Effect of metformin plus tyrosine kinase inhibitors compared with tyrosine kinase inhibitors alone in patients with epidermal growth factor receptor-mutated lung adenocarcinoma A phase 2 randomized clinical trial. *Jama Oncol.* **5** (2019).
56. El-Haggag, S. M., El-Shitany, N. A., Mostafa, M. F. & El-Bassiouny, N. A. Metformin may protect nondiabetic breast cancer women from metastasis. *Clin. Exp. Metast.* **33**, 339–357. <https://doi.org/10.1007/s10585-016-9782-1> (2016).
57. Fan, H. et al. Metformin improves survival in patients with concurrent diabetes and small cell lung cancer: a meta-analysis. *Minerva Endocrinol.* **48**, 214–221. <https://doi.org/10.23736/S2724-6507.21.03289-2> (2023).
58. Reagan-Shaw, S., Nihal, M. & Ahmad, N. Dose translation from animal to human studies revisited. *Faseb J.* **22**, 659–661. <https://doi.org/10.1096/fj.07-9574LSF> (2008).
59. Li, B. et al. Metformin induces cell cycle arrest, apoptosis and autophagy through ROS/JNK signaling pathway in human osteosarcoma. *Int. J. Biol. Sci.* **16**, 74–84. <https://doi.org/10.7150/ijbs.33787> (2020).
60. Di, J., Bo, W., Wang, C. & Liu, C. Ailanthone increases cisplatin-induced apoptosis and autophagy in cisplatin resistance non-small cell lung cancer cells through the PI3K/AKT/mTOR pathway. *Curr. Med. Chem.* **31**. <https://doi.org/10.2174/0109298673315460240816091032> (2024).
61. Zugazagoitia, J. & Paz-Ares, L. Extensive-stage small-cell lung cancer: first-line and second-line treatment options. *J. Clin. Oncol.* **40**, 671. <https://doi.org/10.1200/Jco.21.01881> (2022).

Acknowledgements

This work was supported by the National Natural Science Foundation of China (grant number: 82203366), the Hubei Provincial Natural Science Foundation (grant number: 2022CFB965), the Cultivating Project for Young Scholars at Hubei University of Medicine (grant numbers: 2018QDJZR11 and 2018QDJZR01), the Innovation Research Program for Graduates of Basic Medical College, Hubei University of Medicine (grant numbers: JC2022011, JC2022014, and JC2023009), and the Hubei Provincial Training Program of Innovation and Entrepreneurship for Undergraduates (grant number: S202210929020). We thank the facility centre of the Biomedical Research Institute of Hubei University of Medicine for support with confocal microscopy (Olympus FV3000RS).

Author contributions

Fuyun Ji and Xihua Li conceived the study. Hong Xia, Yi Wu, and Lifeng Wang performed the experiments in vitro. Dandan Liu, Xuejiao Tai, Huzi Zhao, and Dan He designed and conducted animal experiments. Shenyi Zhang, Hao Liu, Yuting Sun, and Hangzhi Liu participated in the data analysis. Xihua Li wrote the manuscript. Fuyun Ji revised the manuscript. All authors critically reviewed the manuscript and approved the final version for publication.

Declarations

Competing interests

The authors declare no competing interests.

Ethical approval

All animal experiments were approved by the Experimental Animal Ethics Committee of Hubei University of Medicine [2022-No.035].

Additional information

Supplementary Information The online version contains supplementary material available at <https://doi.org/10.1038/s41598-025-87537-z>.

Correspondence and requests for materials should be addressed to F.-y.J. or X.-h.L.

Reprints and permissions information is available at www.nature.com/reprints.

Publisher's note Springer Nature remains neutral with regard to jurisdictional claims in published maps and institutional affiliations.

Open Access This article is licensed under a Creative Commons Attribution-NonCommercial-NoDerivatives 4.0 International License, which permits any non-commercial use, sharing, distribution and reproduction in any medium or format, as long as you give appropriate credit to the original author(s) and the source, provide a link to the Creative Commons licence, and indicate if you modified the licensed material. You do not have permission under this licence to share adapted material derived from this article or parts of it. The images or other third party material in this article are included in the article's Creative Commons licence, unless indicated otherwise in a credit line to the material. If material is not included in the article's Creative Commons licence and your intended use is not permitted by statutory regulation or exceeds the permitted use, you will need to obtain permission directly from the copyright holder. To view a copy of this licence, visit <http://creativecommons.org/licenses/by-nc-nd/4.0/>.

© The Author(s) 2025